High-speed tuning of visible laser wavelength using a nanoimprinted grating optical tunable filter

Nien-Tsu Huang,[1] Steven C. Truxal,[1] Yi-Chung Tung,[2] Amy Hsiao,[2] Shuichi Takayama,[2] and Katsuo Kurabayashi[1,3,a)]
[1]*Department of Mechanical Engineering, University of Michigan, Ann Arbor, Michigan 48109, USA*
[2]*Department of Biomedical Engineering, University of Michigan, Ann Arbor, Michigan 48109, USA*
[3]*Department of Electrical Engineering and Computer Science, University of Michigan, Ann Arbor, Michigan 48109, USA*

(Received 10 September 2009; accepted 31 October 2009; published online 24 November 2009)

We report on a microelectromechanical tunable optical filter incorporating strain-tunable nanoimprinted elastomeric grating with a pitch varied by 18%. This device enables tuning of optical fiber-guided laser wavelength between $\lambda=473$ and 532 nm within 0.5 ms by mechanically modulating the pitch with a silicon microactuator. We also demonstrate the use of the device for obtaining two-color images of live/dead-stained cells with the color intensity ratio varied by the actuator voltage applied. The small structure of the device integrated on a silicon chip may be used in portable systems for optical switching and spectroscopy. © *2009 American Institute of Physics*. [doi:10.1063/1.3267083]

Laser wavelength tuning is an important operation for many optical instruments. It finds a wide variety of applications in fiber optical communication,[1,2] spectroscopy,[3,4] and photochemistry.[5] With recent advancements of multicolor fluorescence labeling techniques for biological studies,[6,7] a demand for the ability to tune laser wavelength in the visible band grows even stronger. In fluorescence spectroscopy and imaging, laser wavelength tuning is often achieved using tunable optical filters, such as acousto-optical tunable filters and liquid crystal tunable filters.[8] However, the relatively large-volume structures of these filters make them undesirable for the use in optofluidic lab-on-a-chip settings and point-of-care portable module systems.

Several miniaturized silicon microelectromechanical systems (MEMS)-based tunable gratings have been developed and demonstrated for high-speed wavelength tuning in the infrared band or in the visible band at reduced spectral resolution.[9–11] Toward the goal of MEMS-based high-resolution visible wavelength tuning, our previous study[12] developed a nanoimprinted polydimethylsiloxane (PDMS) elastic pitch-variable grating mechanically tuned by on-chip silicon comb drive electrostatic actuators. But the device's small pitch variation range of 2.5% resulting in narrow bandwidth tuning (15 nm at $\lambda=558$ nm) limits its practical use for biofluorescent applications that involve significant spectral shifts of light.

In this letter, we demonstrate high-speed two-color laser switching using a polymer-on-silicon MEMS grating optical tunable filter (GOTF) device with a much larger pitch variation range. The GOTF device is fabricated using a method named the multilevel soft lithographic lift-off and grafting (ML-SLLOG).[13] The ML-SLLOG process involves (1) fabrication of comb drives on a silicon-on-insulator (SOI) wafer, (2) soft lithography[14] and lift-off of a three-dimensional PDMS microstructure, and (3) grafting of the PDMS microstructure onto the SOI patterns based on microassembly assisted by surface tension at an air-water interface.[15] The surfaces of the PDMS and silicon structures are both activated by oxygen plasma treatment to promote their permanent bonding in step (3).

Figures 1(a) and 1(b) show the SEM and optical images of device(s). Each GOTF device occupies a 3 mm × 3 mm area. The 250 μm long PDMS bridge, shown in the inset of Fig. 1(a), has a surface feature of 350 grating lines with an initial period of 700 nm and a height of 350 nm. The first order grating efficiency for this feature is calculated to be 18%–23% for $\lambda=470-530$ nm using GSOLVER software (Grating Solver Development Co., Allen, Texas). Our previous study[15] shows that the PDMS-silicon bond is strong enough to sustain stretching actuation at strain as large as 40% and that more than 100 million cycles of operation re-

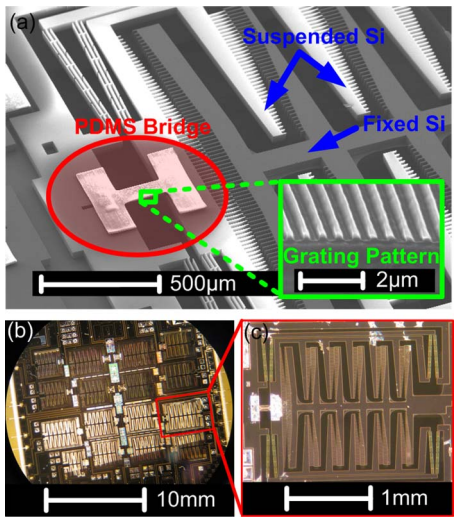

FIG. 1. (Color online) Images of the nanoimprinted grating optical tunable filter (GOTF) device. (a) SEM image of the entire device consigning of a 250 μm long, 150 μm wide, 15 μm thick PDMS grating microbridge with 700 nm nominal pitch, and MEMS silicon comb drive electrostatic actuators. (b) Optical image of 16 device arrays on a 2×2 cm^2 die area. (c) Optical image of the whole device unit.

a)Author to whom correspondence should be addressed. Electronic mail: katsuo@umich.edu.

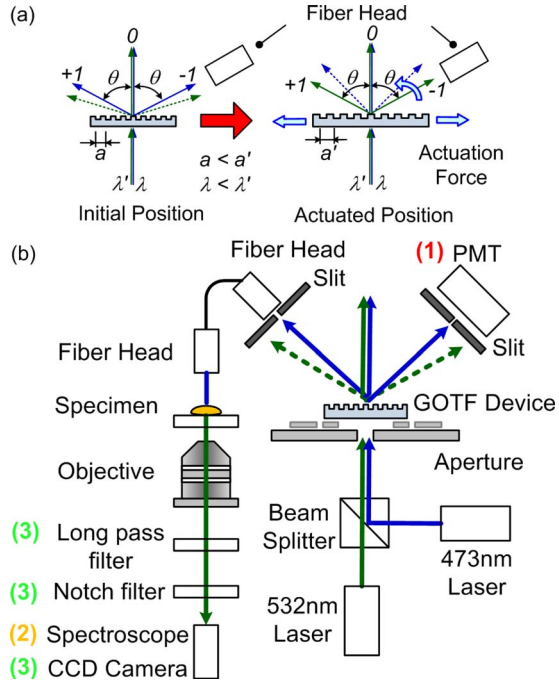

FIG. 2. (Color online) Device operation and characterization. (a) Working principle of the GOTF device. The period of the grating changes from a to a' when subjected to mechanical strain. The wavelength of the first order diffraction at the same diffraction angle θ shifts from λ to λ'. The wavelength shift of the first order diffraction at the angle θ is tuned by the actuation voltage V_a applied to the comb drives. (b) Experimental setups incorporating the GOTF for (1) dynamic optical switching bandwidth measurement, (2) excitation spectrum measurement, and (3) live/dead PC3 cell two-color imaging.

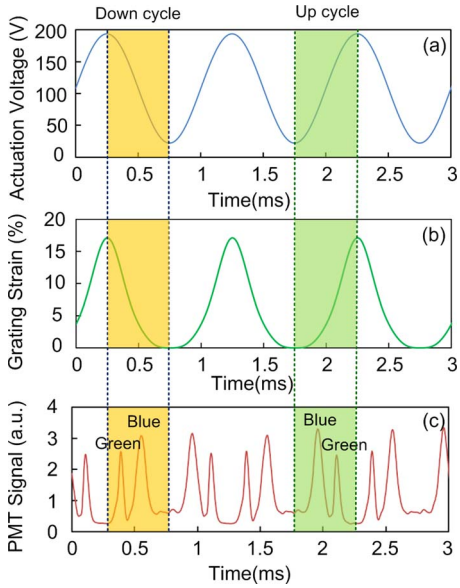

FIG. 3. (Color online) Results for high-speed ALEX using the GOTF device. (a) Sinusoidal actuation voltage applied to the comb drives of the GOTF device. (b) Grating strain. (c) PMT signal.

sult in no performance degradation for a device fabricated in the same fashion as the one studied here. The GOTF yields large mechanical tunability of the grating pitch as a result of its long-distance (>80 μm) movements. To achieve a larger grating pitch variation range, the comb drive design incorporates silicon springs with a tilted folded-beam and a series of tapered arrangements of electrode fingers. It serves to minimize (1) nonlinear spring effects and (2) electrostatic instability resulting from pull-in force in the direction perpendicular to the comb drive motion, both of which accompany the large movement of the suspended silicon structure.[16,17]

The wavelength tuning is performed by varying the initial PDMS grating pitch a with the silicon comb drives driven by the actuation voltage V_a, [Fig. 2(a)]. Here, the optical filtering is achieved by spatially blocking light other than the one diffracted to a targeted optical path. To demonstrate the wavelength tuning speed, spectral resolution, and wavelength speed of the GOTF device, we implemented the device into an experimental setup shown in Fig. 2(b), where blue (λ=473 nm) and green (λ=532 nm) color laser lights (BWB-475–4E, B&W TEK and BWB-532–10E, B&W TEK, respectively) pass through the GOTF. We apply a sinusoidal actuation voltage of 20–180V at 1 kHz to the GOTF comb drives [Fig. 3(a)]. A photomultiplier tube (PMT) (H8249–12, Hamamatsu Photonics) selectively captures a laser signal switched by the sinusoidal actuation voltage [Setup 1 in Fig. 2(b)]. Figure 3(b) shows strain introduced to the grating by the sinusoidal actuation voltage. It is derived from the change in the first order diffraction angle θ measured for monochromatic incident light at λ=532 nm using a position sensitive diode (C4674, Hamamatsu Photonics). Figure 3(c) shows a PMT signal with two peaks corresponding to the two-color laser light inputs at a wavelength tuning range of 460–540 nm. We obtain the spectral resolution of $\Delta\lambda$=4 nm at 473 nm and $\Delta\lambda$=8 nm at 532 nm from the full width half maximum of the signal. The result demonstrates the device's high-speed (1 kHz) passband wavelength tuning capability.

Subsequently, we show that the GOTF can be operated in a fluorescent microscope (Nikon Eclipse TS100, Nikon Inc.) setting [Setup 2 in Fig. 2(b)]. Here, an aperture of 1 mm diameter is placed in front of the device before light beam reaches the grating to eliminate excessive light and to reduce optical noise. A fiber with a 1000 μm diameter core and NA=0.22 (A57–746, Edmund Optics.) is used to capture the excitation light diffracted by the grating. Figure 4(a) shows the excitation spectrum as a function of V_a, measured by the optical spectrometer (USB4000, Ocean Optics) coupled with a 10× objective lens [Setup 2 in Fig. 2(b)]. At V_a=20 V, only the blue excitation is guided onto the specimen stage while green excitation is blocked. With V_a increased to 120 V, the blue excitation intensity significantly drops more than three orders of magnitude after reaching the maximum value at V_a=40 V. At V_a=150 V, the green excitation intensity increased rapidly with the increasing voltage. At V_a =175 V, green excitation intensity reaches the maximum value with a signal-to-noise ratio nearly 4×10^3. Tuning the actuation voltage allows us to adjust the ratio between the blue and green excitation laser intensities in a programmable manner, which would be useful for dual-excitation ratiometric dye detection.[18]

Finally we demonstrate voltage-controlled modulation of the intensity ratio of two-color fluorescent emissions from a biological sample with the GOTF [Setup 3 in Fig. 2(b)]. A 500 nm long pass filter (S-003767, Chroma) and a 532 nm notch filter (NF01–532U-25, Semrock) are used to eliminate the excitation lasers. Here, we use PC-3 prostate cancer cells maintained in complete media consisting of RPMI-1640 (61870, Gibco) supplemented with 10% (v/v) fetal bovine serum (FBS, 10082, Gibco), and 1% (v/v) antibiotic-

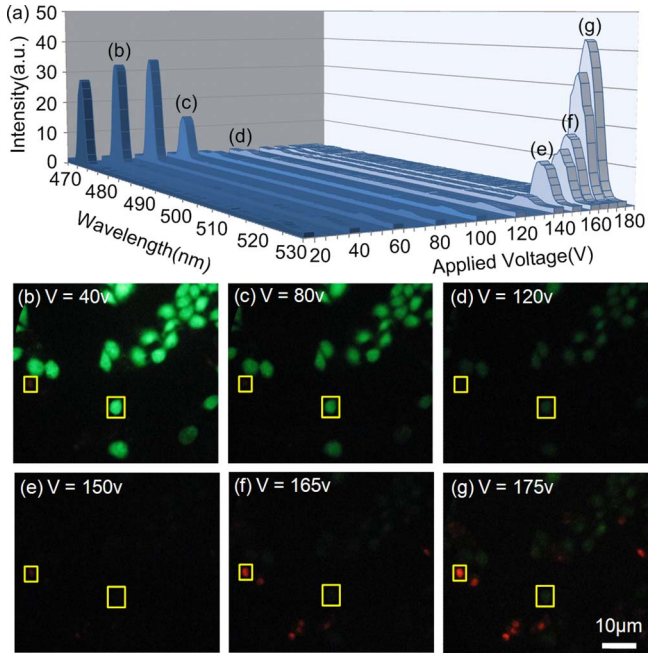

FIG. 4. (Color online) Results for two-color live/dead PC3 cell imaging. (a) Excitation spectrum as a function of the actuation voltage applied to the GOTF device. [(b)–(g)] Sequence of images corresponding to the excitation spectrum in (a). The emission intensities are measured for the areas marked with a square frame.

antimycotic (15240, Invitrogen). The cells are stained by LIVE/DEAD Viability/Cytotoxicity Kit for mammalian cells (L-3224, Invitrogen). Calcein AM and Ethidium homodimer-1 diluted in PBS to a final concentration of 1 and 2 μM, respectively, are added to the PC-3 cells and incubated for 30 min at 37 °C.

Figures 4(b)–4(e) constitute an image sequence that shows adjustable excitation of the stained cell by varying V_a. Using IMAGEJ software (National Institute of Health), the intensity of a single cell with the live (green emission) or dead (red emission) stain is obtained. At V_a=40 V, the green/red intensity ratio is 6.08, indicating dominance of the emission of the live stain cells excited by the blue laser. At V_a between 120 and 150 V, a green/red ratio drop (alternatively, a red/green ratio increase) is observed in response to the switching of the excitation color. At V_a=165 V, the green/red ratio is 0.26, which shows most dead stain cells are excited by the green laser excitation. At V_a=175 V, the green/red ratio slightly increases because of the bleedthrough, where both the live/dead stains are excited by the green laser due to the overlap of their excitation spectra in the wavelength band. With this voltage-controlled wavelength tuning method, we can adjust the wavelength of an excitation light source *in situ* during detection of multicolor fluorescent labels.

In summary, we have demonstrated two-color laser wavelength tuning by an optical filtering device incorporating a pitch-variable elastic grating integrated on a silicon chip. This grating device can achieve wavelength tuning to alternate fiber-guided laser wavelength between λ=473 and 532 nm at 1 kHz dynamic bandwidth. Our work integrates this device and the lasers into a fluorescent microscope to modulate the two-color emission intensity ratio of an image of live/dead stained PC3 prostate cancer cells by a factor of 30 with the device's grating pitch varied by 18%. Like other conventional tunable optical filter devices, this device may also find its utility in alternating laser excitation (ALEX) or spectroscopy for capturing dynamic biological interactions.[19,20] Using lithography based batch fabrication, we can construct 16 GOTF device arrays in a 2×2 cm^2 die area. Coupled with multiple optical fiber channels, the device arrays could enable massively parallel ALEX and spectroscopic measurements for lab-on-a-chip systems.

This work is supported by NSF (Grant No. ECCS-0601237), NIH (Grant No.HG004653), NIH/NIBIB training grant to AH (Grant No. T32 EB005582), and the University of Michigan, Mechanical Engineering Graduate Fellowship.

[1] A. Banerjee, Y. Park, F. Clarke, H. Song, S. Yang, G. Kramer, K. Kim, and B. Mukherjee, J. Opt. Netw. **4**, 737 (2005).
[2] J. A. Alvarez-Chavez, A. Martínez-Rios, I. Torres-Gomez, and H. L. Offerhaus, Laser Phys. Lett. **4**, 880 (2007).
[3] G. Lammel, S. Schweizer, S. Schiesser, and P. Renaud, J. Microelectromech. Syst. **11**, 815 (2002).
[4] H. Sato, S. Wada, and H. Tashiro, Appl. Spectrosc. **56**, 1303 (2002).
[5] M. L. Gostkowski, R. Allen, M. L. Plenert, E. Okerberg, M. J. Gordon, and J. B. Shear, Biophys. J. **86**, 3223 (2004).
[6] Y. Santoso, L. C. Hwang, L. L. Reste, and A. N. Kapanidis, Biochem. Soc. Trans. **36**, 738 (2008).
[7] J. Ross, P. Buschkamp, D. Fetting, A. Donnermeyer, C. M. Roth, and P. Tinnefeld, J. Phys. Chem. B **111**, 321 (2007).
[8] N. Gat, Proc. SPIE **4056**, 50 (2000).
[9] H. Sagberg, M. Lacolle, I. Johansen, O. Lvhaugen, R. Belikov, O. Solgaard, and A. S. Sudb, IEEE J. Sel. Top. Quantum Electron. **10**, 604 (2004).
[10] X. Li, C. Antoine, D. Lee, J. Wang, and O. Solgaard, J. Microelectromech. Syst. **15**, 597 (2006).
[11] Y. Wang, Y. Kanamori, T. Sasaki, and K. Hane, J. Micromech. Microeng. **19**, 025019 (2009).
[12] Y.-C. Tung and K. Kurabayashi, Appl. Phys. Lett. **86**, 161113 (2005).
[13] Y.-C. Tung and K. Kurabayashi, *Proceeding of 18th IEEE International Conference on Microelectromechanical Systems* (IEEE, Piscataway, New Jersey, 2005), pp. 243–246.
[14] S. Y. Chou, P. R. Krauss, and P. J. Renstrom, J. Vac. Sci. Technol. B **14**, 4129 (1996).
[15] S. C. Truxal, Y.-C. Tung, and K. Kurabayashi, J. Microelectromech. Syst. **17**, 393 (2008).
[16] G. Zhou and P. Dowd, J. Micromech. Microeng. **13**, 178 (2003).
[17] J. D. Grade, H. Jerman, and T. W. Kenny, J. Microelectromech. Syst. **12**, 335 (2003).
[18] T. Fukano, S. Shimozono, and A. Miyawaki, Biochem. Biophys. Res. Commun. **340**, 250 (2006).
[19] A. N. Kapanidis, N. K. Lee, T. A. Laurence, S. Doose, E. Margeat, and S. Weiss, Proc. Natl. Acad. Sci. U.S.A. **101**, 8936 (2004).
[20] C. Hesch, J. Hesse, and G. J. Schütz, Biosens. Bioelectron. **23**, 1891 (2008).